Since January 2020 Elsevier has created a COVID-19 resource centre with free information in English and Mandarin on the novel coronavirus COVID-19. The COVID-19 resource centre is hosted on Elsevier Connect, the company's public news and information website.

Computers, Environment and Urban Systems 34 (2010) 204–215

Contents lists available at ScienceDirect

Computers, Environment and Urban Systems

journal homepage: www.elsevier.com/locate/compenvurbsys

Spatial–temporal transmission of influenza and its health risks in an urbanized area

Liang Mao *, Ling Bian [1]

Department of Geography, University at Buffalo, State University of New York, Amherst, NY 14261, USA

ARTICLE INFO

Article history:
Received 26 September 2009
Received in revised form 11 March 2010
Accepted 11 March 2010

Keywords:
Spatial–temporal dynamics
Influenza transmission
Urban environment
Individual-based modeling

ABSTRACT

Cities and urban areas play an important role in fostering influenza transmission, often leading to epidemics and even pandemics. Although there is growing literature on influenza transmission at national and international scales, little attention has been paid to a city scale. This article aims to understand the spatial–temporal transmission of influenza and identify its health risks in the urbanized area of Buffalo, New York. An individual-based spatially explicit model is established to replicate an urban contact network, and simulate influenza epidemics. The resulting epidemic curves and infection intensity maps are used to analyze the transmission dynamics, possible contributing factors, and high-risk places and times. The results indicate that the city-wide transmission of influenza can be described by five stages: local growth, expansion, fast city-wide growth, slow city-wide growth, and fade-out. The places and times associated with higher risk are closely related to spatial heterogeneity in the population, and travel behaviors of individuals. Interestingly, these high-risk places and times are insensitive to where infection sources are introduced. This research suggests that high-risk places can be pre-identified as control targets using census and land use data. In addition, a better understanding on the city-wide travel of individuals is critical for designing proper timelines for influenza control. These suggestions will be valuable for local health agencies as they prepare to combat new waves of H1N1 influenza.

1. Introduction

Every year in the United States, influenza (commonly known as flu) is responsible for more than 30,000 deaths and about 200,000 hospitalizations (Thompson et al., 2004). The total economic burden of influenza epidemics amounted to $87.1 billion/year (Molinari et al., 2007). In recent years, influenza has obtained unprecedented attention due to widespread occurrence of novel influenza viruses, such as the bird flu and H1N1 flu. A major public health concern is the possibility of a pandemic, which could be as severe as the 1918 Spanish flu (Webby & Webster, 2003). This great concern has motivated scientists and health policy makers to model influenza epidemics and predict transmission dynamics (Coburn, Wagner, & Blower, 2009).

Influenza is an infectious disease transmitted from individual to individual through physical contacts. The transmission is often fostered and amplified in cities and urban areas. The dense human contacts in a city form fast and uncontrolled channels for transmission (Meade & Earickson, 2005). In addition, cities can serve as hubs that transmit diseases to small "satellite" towns, resulting in regional or even global pandemics (Grenfell, Bjornstad, & Kappey, 2001). Although the importance of cities is widely recognized, little research has been devoted to modeling and understanding the city-wide influenza transmission. A possible challenge is to represent and analyze much detailed information at such a small scale. In recent literature, there has been seen a few efforts to model city-scale disease epidemics, such as the EpiSims model by Eubank et al. (2004), and the BioWar model by Carley et al. (2006). These studies have been focused on modeling issues at the city scale, but little attention has been paid to the spatial–temporal transmission of influenza, possible factors contributing to transmission, and resultant urban health risks.

For these reasons, the objectives of this article are to understand the spatial–temporal transmission of influenza, and identify its health risks in the urbanized area of Buffalo, New York. An individual-based spatially explicit model is established to represent an urban contact network. Based on such network, infection sources are introduced with different patterns and corresponding influenza epidemics are simulated. The transmission of influenza over time and space is analyzed, and potential places and times of high risk are identified. The remainder of this article is organized into the following sections. The second section introduces the individual-based modeling approach used in this study. The third section describes the urbanized area of Buffalo and the simulation model for influenza transmission. The two sections that follow present and discuss the simulation results, respectively. The last section concludes the article and discusses its implications.

* Corresponding author. Tel.: +1 (716) 348 0836; fax: +1 (716) 645 2329.
E-mail addresses: liangmao@buffalo.edu (L. Mao), lbian@buffalo.edu (L. Bian).
[1] Tel.: +1 (716) 645 0484; fax: +1 (716) 645 2329.

0198-9715/$ - see front matter © 2010 Elsevier Ltd. All rights reserved.
doi:10.1016/j.compenvurbsys.2010.03.004

2. An individual-based modeling approach for epidemiology

During the past decade, the individual-based approach began to gain momentum in modeling a variety of infectious diseases, such as influenza, smallpox, severe acute respiratory syndrome (SARS), foot and mouth disease (FMD), and others (Eubank et al., 2004; Huang, Sun, Hsieh, & Lin, 2004; Keeling et al., 2001; Longini et al., 2005). These individual-based models use a bottom-up approach, which starts with discrete individuals of a population, and tries to understand how the population's properties emerge from interactions among individuals (Grimm & Railsback, 2005). This approach offers three advantages for modeling disease transmission. First, the heterogeneity of both individuals and their interactions can be explicitly represented, as can the subsequent heterogeneity in disease transmission (Keeling, 1999; Koopman & Lynch, 1999). Second, the randomness of disease infection between a pair of individuals can be captured as a stochastic process. Third, by aggregating individual infections, the outcome of disease transmission can be studied at multiple scales, such as the community, city, national and international scales. These three advantages bring the epidemic modeling closer to reality than other traditional models. However, the increased realism demands more assumptions to be made and more parameters to be estimated, bringing more complexity in modeling (Judson, 1994; Koopman, 2002).

In many individual-based epidemic models, the concept of network is often included to represent contacts among individuals (Bian, 2004; Eubank, 2005). Conceptually, the network is composed of nodes and links, where nodes represent individuals and links represent direct contacts among individuals (Wasserman & Faust, 1994). Nodes can have attributes, such as a finite number of links and an infection status. Links also have a set of attributes, including the closeness and duration of the contact, and the likelihood of infection. The diseases are transmitted through links over the population (Keeling & Eames, 2005).

In recent years, there has been a rising number of individual-based spatially explicit models for disease epidemics at the national and international scales, including the models for the United States (Germann, Kadau, Longini, & Macken, 2006; Halloran et al., 2008), for Great Britain (Riley & Ferguson, 2006), and for South Asia (Ferguson et al., 2005; Longini et al., 2005). In these macro-scale models, the fundamental geographic unit is a community, which can be either a census tract or a pre-defined square area. Individuals are assigned to different communities to satisfy a set of real demographic distributions, such as the distributions of age, gender, and household size. Nationwide workplace data and traveling statistics are utilized to simulate individual travel behavior within and between communities, often following a distance-decay law. These models successfully replicate wave-like and hierarchical diffusion patterns that occur in geographically extensive areas. However, by covering such larger geographic areas, these models often simplify or neglect the detailed information within a city, such as the specific locations of households and workplaces, the urban transportation network, and the daily activities of individuals. These models, therefore, may be less useful for planning influenza control in individual cities.

Currently, quite a few individual-based models have been proposed at the city scale. These models include: the EpiSims model (Eubank et al., 2004) for smallpox in Portland, Oregon; the BioWar simulation of an influenza epidemic in Norfolk, Virginia (Lee, Bedford, Roberts, & Carley, 2008); and the activity-based model for influenza in Eemnes, Netherlands (Yang, Atkinson, & Ettema, 2008). These cities are modeled using specific locations of households, workplaces, schools, health facilities, etc. Each individual has a set of demographic, socio-economic, and behavioral characteristics that are estimated from census data and behavioral surveys. By taking a range of daily activities (such as work, study and shopping), individuals move between several locations, both exposing themselves to infectious diseases within these locations and transporting diseases between locations (Eubank et al., 2004).

Compared to the macro-scale models, these city-scale models include such detailed descriptions that every individual can be identified at a specific location and time. The information about who infects whom, and where and when the infection happens can be traced and recorded. The increased details, however, introduce more complexity to the model, and thus only a few city-scale models exist so far. Another issue is that few of these city-scale models have been used to explore the potential patterns, contributing factors, and health risks of influenza transmission. The relevant literature mainly reports model establishment and tests control strategies, but influenza transmission itself is under-studied. This study aims to fill this knowledge gap using an individual-based city-scale model.

3. Study area and simulation model

3.1. Study area

The urbanized area of Buffalo is located at the western end of New York State, and on the eastern shore of Lake Erie (Fig. 1a). Geographically, the study area is relatively separated from other urbanized areas, because it is surrounded by great lakes and rural areas. The nearest urbanized area, Rochester, New York, is about 120 km to the east. According to 2002 travel survey by Greater Buffalo-Niagara Regional Transportation Council (GBNRTC, 2002), most people living in this area take their daily activities within it. For these reasons, the study area can be treated as a closed system, where an influenza epidemic may develop with little outside influence. If an epidemic were to reach this area, the most likely situation would be that the epidemic had already started elsewhere, and the virus would be introduced by infected travelers.

According to the US Census (2000), the study area encloses a population of 985,001 individuals in 400,870 households (in 967 census block groups and 12,328 census blocks). The age structure indicates that approximately 37.5% of the population is at a high risk of influenza infection, including children younger than 18 years (24.1%) and seniors older than 64 years (13.4%) (Heymann, 2004). In addition, the study area contains 36,839 business locations, according to published business databases from ReferenceUSA, Inc (2009). These business locations include: offices, factories, schools, service places, health care facilities, etc., and they are classified by the North American Industry Classification System (NAICS). Relevant to this study, individuals may have contact with others in these households and business locations, transmitting influenza virus within and between these locations.

The study area has a clear spatial structure with three zones: a central business district (CBD), a transition zone, and suburbs (Knox & Marston, 2004). The delineation is based on the densities of population, households, businesses, and the layout of road system. As shown in Fig. 1b, the CBD covers an area of 42.0 km^2, and consists of downtown areas in the city of Buffalo and the city of Niagara Falls. Downtown Buffalo is enclosed by Interstate Highway 190, and State Routes 33 and 198, while Downtown Niagara Falls is surrounded by State Route 61 and Robert Moses Parkway. The CBD is characterized by its significantly higher densities of residents, households, and businesses than the other two zones (Table 1). The transition zone is adjacent to the CBD, and is enclosed within Interstate Highways 290, 190 and 90, and State Route 61. With an area of 144.6 km^2, this zone has the second highest densi-

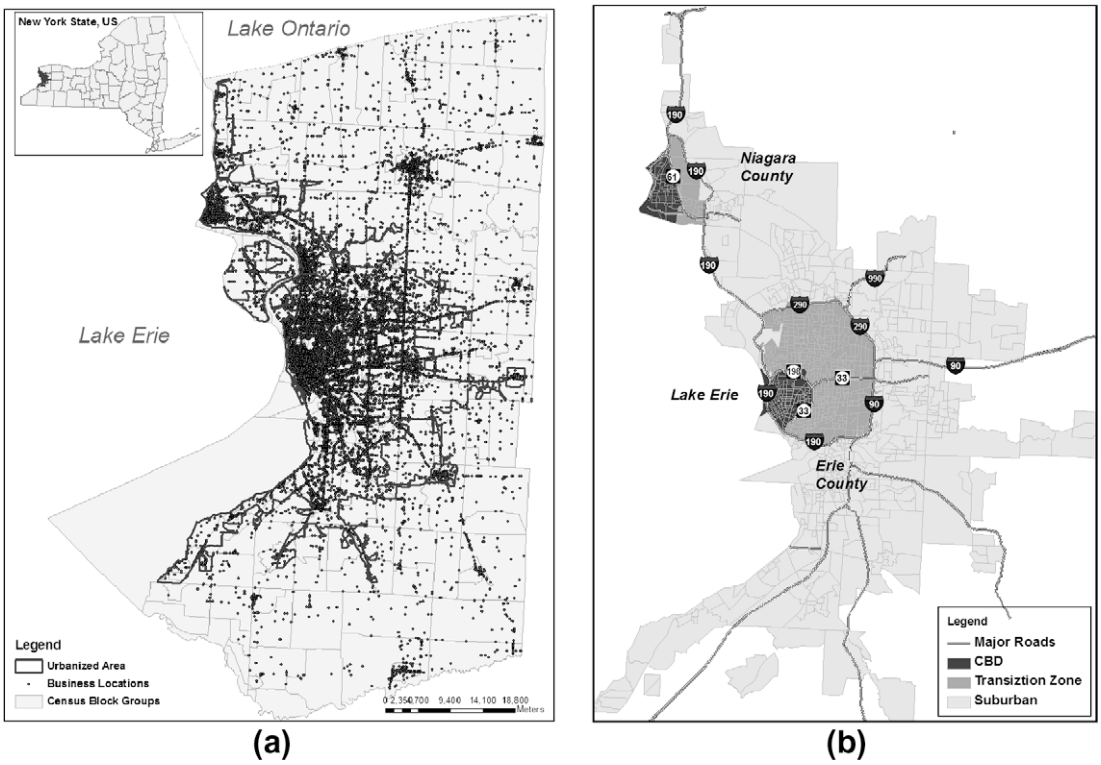

Fig. 1. (a) The spatial location of Buffalo urbanized area (the inset map), the census block groups and business locations. (b) The three-in-one spatial structure of the Buffalo urbanized area.

Table 1
The zonal distributions of population, households, and business in the study area.

Zones	CBD	Transition zone	Suburbs
Total residential population	115,850	304,030	565,121
Total households	49,951	127,147	223,772
Total business locations	6227	9746	20,866
Density of residential population	2758.33	2102.56	53.62
Density of households	1189.30	879.30	21.30
Density of business locations	148.26	67.40	1.98

*Area unit: km^2.

ties of residents, households, and businesses. The rest of the urbanized area is the suburbs, which covers a large area of 10,538.1 km^2. The suburbs are featured by the largest numbers of residents, households, and businesses, but their densities are the lowest. This spatial structure is considered later for seeding infection sources and describing disease transmission patterns.

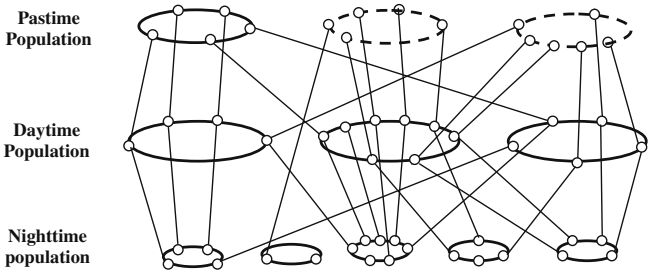

Fig. 2. The conceptual framework of the urban social network for influenza transmission (revised based on Bian (2004)). Ovals represent homes at the nighttime, workplaces at the daytime, or service places/neighbor households at the pastime. Small circles on an oval represent individuals who interact with one another within a location. The solid-line ovals denote close contacts among individuals, while the dash-line ovals denote occasional contacts. A straight line between the three time periods represents the travel of an individual, and links an identical individual at different locations.

3.2. Simulating an urban contact network

To simulate influenza transmission, an urban contact network is modeled first as a basis. A conceptual network model proposed by Bian (2004) is used to represent individuals, contacts among individuals, and how these contacts change with times and locations. The contacts among individuals are assumed to take place during three time periods in a day and at four types of locations (Fig. 2). The three time periods include the daytime (e.g., 9 am–6 pm), pastime (e.g., 6 pm–12 am), and nighttime (e.g., 12 am–9 am), while the four types of locations include homes, workplaces, service places, and neighbor households. Under this spatial–temporal frame, individuals may have two types of contacts: close contacts and occasional contacts. Close contacts happen at homes, workplaces, and neighbor households, where an individual has contact with all the other individuals in the same location. Occasional contacts happen in service places, where an individual only has contact with a limited number of individuals. These spatial–temporally dependent contacts link individuals into a population-wide network.

The urban contact network is established based on the simulation of three populations corresponding to the three time periods: a nighttime population at homes, a daytime population at workplaces, and a pastime population at service places or neighbor households (Fig. 2). The three populations represent the same set of individuals at different locations and time periods of a day. To create the three populations and establish links between populations, each of the 985,001 individuals is a modeling unit with a set of attributes (Fig. 3). Individuals are assigned to specific locations of their homes, workplaces, service places and neighbor households, and are assumed to travel between these four types of locations through real road system.

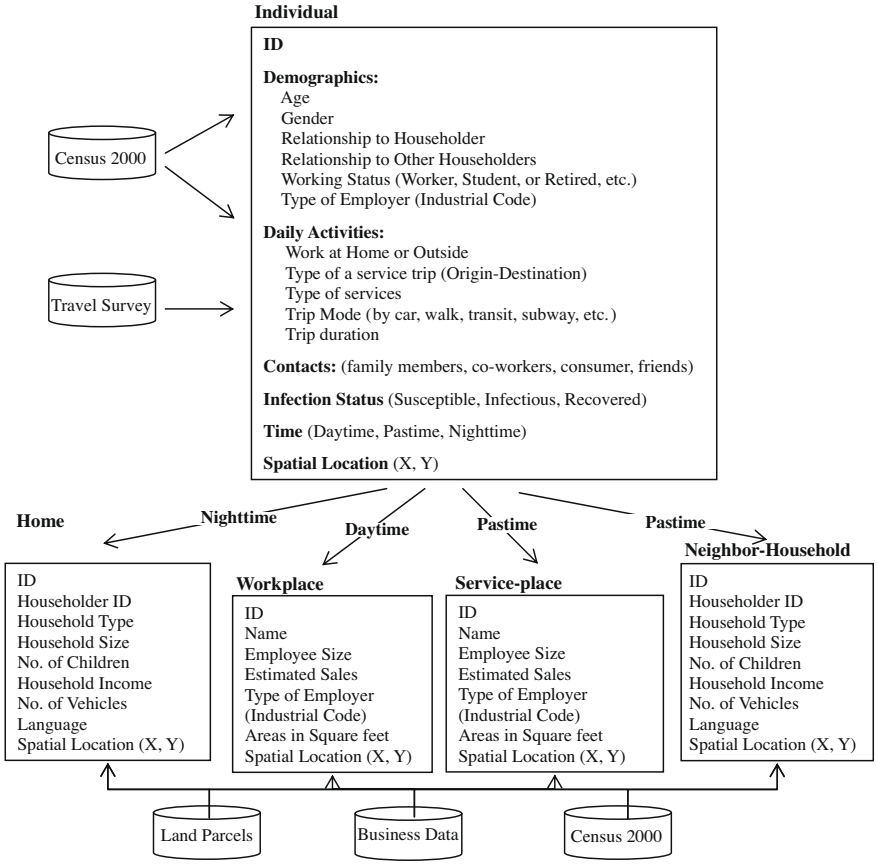

Fig. 3. The assignment of individuals to households, workplaces, service places and neighbor households based on the attribute and spatial information of individuals.

The 2000 census data (primarily Summary File 3) and land parcel data from New York State GIS Clearinghouse (2009) are used for simulating the nighttime population at homes. Two sets of information are extracted from the aggregated census data at a block group level, one for individuals and the other for homes (or more generally households), as shown in Fig. 3. Using algorithms developed by Bian et al. (2008), table cross-referencing and Monte–Carlo simulation are performed to fit the modeled distributions to real demographic distributions. The spatial distribution of households, expressed by (x, y) coordinates, is estimated based on the number of households within a census block, and the centroids of land parcels in that block.

Three sets of information are used to simulate the daytime population at workplaces: the 2000 census data, published business databases, and attributes associated with previously simulated individuals and households. While the business databases provide information about workplaces (including spatial locations), the census data and the previously created attributes of individuals and households help assign individuals to these workplaces (Fig. 3). A worker is randomly assigned to a workplace that satisfies two criteria (Bian et al., 2008). First, the employer type of the workplace from the business databases should match the employer type of the worker from the census data. Second, the shortest distance between the home and workplace in the real road system should match the trip distance to work estimated from the census data (trip duration to work $\times$ speed of a trip mode). Unlike ordinary workers, school-aged individuals in each household are assigned to a nearest school as their workplace. To differentiate the weekdays and weekends, individuals are not assigned to work at weekends except those who work in service-oriented businesses. This completes the daytime population at workplaces and links the nighttime population at homes to the daytime population.

The simulation of pastime population at service places and neighbor households is based on three sets of information. The first set is detailed travel survey data from GBNRTC, providing information about types and frequencies of services needed. The second is a subset of workplaces that are identified as service places based on their NAICS code (8109 out of 36,839 workplaces). The third is the attributes for individuals and households created for the nighttime and daytime populations. Using the frequency statistics in travel survey as constraints, the total number of trips for a household is first determined. The trips of a household are then allocated to workers in the household and then other members of the household. Each trip is assigned, according to frequency statistics, with a trip mode, a trip duration, one of three types of ser-

Table 2
The types of services, examples and corresponding NAICS in simulation.

Service type	Examples	NAICS
Shop/eat out	Grocery store, drug store	44: Retail trade
	Department store	45: Retail trade
	Fast food, restaurant, bar	722: Food service
Recreation	Movies, sports	71: Art, entertainment, recreation
	Music concert	
Banking/personal business	Banking	5221: Bank
	Barbershop/fitness	812: Personal business
Pick up/drop off	School or childcare	6111: Elementary school 6244: Child care
Social	Visit other families	N/A

vice trips (workplace-to-service, home-to-service, and service-to-service), and one of five types of services (Table 2). Given a type of service trip and a type of service, the model assigns an individual to a service place or a neighbor household that matches the trip distance (speed of trip mode × trip duration) (Bian et al., 2008). In this manner, a set of attributes regarding pastime activities of individuals can be generated, as shown in Fig. 3. These activity attributes help create the pastime population and link it to the other two populations.

The establishment of the three linked populations forms a spatially explicit and temporally dynamic contact network. The contacts among individuals within a location cause the local transmission of influenza, while the travel of individuals between the four types of locations leads to spatial dispersion of influenza.

3.3. Simulating influenza transmission

The transmission of influenza is simulated by changing infection status of every individual over time. An individual can take one of four infection status at a given time, i.e., susceptible, latent, infectious, or recovered (Anderson & May, 1992). The progress of infection status follows a series of discrete events in the natural history of influenza (Fig. 4). At some point in time, a susceptible individual comes into the latent status after receiving influenza virus. The receipt of infection starts a 2-day latent period, during which influenza develops internally and cannot be transmitted. At the end of the latent period, the individual becomes infectious and can transmit influenza to other susceptible individuals. The length of infectious period varies from 4 to 7 days depending on the age or health status of the individual (Heymann, 2004). One day after being infectious, this individual may develop symptoms, or otherwise remain asymptomatic. Finally, this individual recovers from influenza and develops immunity for the remaining period of the epidemic.

Among these influenza-related events, the receipt of infection through one contact is simulated base on a probability of infection $p = E_{contact} \times I_{age}$. Here, $E_{contact}$ is the effectiveness of a contact for infection, which is related to closeness and duration of the contact (Yang & Atkinson, 2008). This study simply standardizes the effectiveness of close contacts $E_{close\_contact}$ to one, while the effectiveness of occasional contacts $E_{occasional\_contact}$ is a relative number less than one. I_{age} is termed as age-specific infection rate, and expressed by a real number between [0,1]. It can be interpreted as a conditional probability of infection given $E_{contact} = 1$ and a specific age group of the receiver. For given I_{age} and $E_{contact}$, the probability p can be estimated and the Monte–Carlo method is used to determine whether an infection event will happen or not.

For a more realistic simulation, a background immunity is created by immunizing 62.7% of seniors (older than 64 years), 15.6% of adults (between 18 and 64 years), and 17.9% of children (younger than 18 years), according to reported national immunization coverage (Euler et al., 2005; Molinari et al., 2007). This will result in overall 24% of the population being immunized. In addition, the simulation assumes that 50% of infectious individuals will develop symptoms, following the assumption by Ferguson et al. (2005). Only these symptomatic individuals can be identified as influenza cases. A proportion of these symptomatic individuals may also withdraw to home. Specifically, all symptomatic children are assumed to withdraw to home, because they are often cared by parents at homes. Thirty-three percent of symptomatic adults will withdraw to home based on reported percentage in a health behavior survey (Metzger, Hajat, Crawford, & Mostashari, 2004). All symptomatic seniors will withdraw to home according to related empirical studies (Stoller, Forster, & Portugal, 1993).

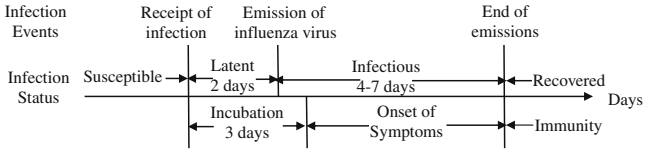

Fig. 4. The infection events, periods and status in the natural history of influenza.

The influenza epidemic is simulated for 120 days, roughly a typical influenza season (from November to February). To initialize the epidemic, five infectious individuals, as infection sources, are seeded into the study area on the first day of the simulation. For a comprehensive analysis, four seeding scenarios are devised based on the aforementioned three-in-one urban structure. Specifically, the five infection sources are randomly distributed: (1) in the entire study area, (2) only in the CBD (e.g., at bus terminals), (3) only in the transition zone (e.g., at local medical centers), and (4) only in the suburbs (e.g., at airports). The influenza epidemic is simulated over 50 realizations under each scenario, resulting in a total of 200 (50 × 4) realizations.

3.4. Description of spatial–temporal transmission dynamics

For each of the four seeding scenarios, the temporal sequence of transmission is described by an epidemic curve that depicts the number of daily new cases during the course of the epidemic (Gordis, 2000). The peak time and the number of new cases at the peak time are two major characteristics of the curve. To reduce the randomness, the epidemic curve and two associated characteristics are estimated by averaging 50 model realizations. To display the spatial spread of influenza, infection intensity maps are created by the following three steps. First, every infection event occurring in a given time interval is plotted as a point at the location of infection, such as the home, workplace, service place, or neighbor household. Second, the study area is divided into a cell grid for subsequent estimation. The reason for rasterization is because plotting tens of thousands of points produces unclear spatial patterns, while rasterization helps provide a clear and reasonable representation. Third, a kernel density function is used to estimate the magnitude of new infections occurring within every cell during a time interval, i.e., the infection intensity at a cell location. A high-intensity value indicates that the corresponding cell location is undergoing a rapid growth in the number of infections.

The spatial spread of influenza, then, can be displayed by creating a series of infection intensity maps for every 20 days of the total 120-day simulation. The cell size is set to 50 m × 50 m because it approximates the average extent of a land parcel (the estimated extent is 47 m × 47 m). In this sense, one or more cells can cover the spatial extent of a location and produce sufficient detail for subsequent analysis. The intensity value at every cell location is estimated by a kernel density function, and is averaged over 50 model realizations. The bandwidth of the kernel is set to 1500 m to produce an optimal balance between clear patterns and biases introduced by the function.

4. Simulation results and analysis

4.1. Model calibration and validation

The simulation model is calibrated and partially validated by established literature. For the urban contact network, the simulated populations in the nighttime, daytime, and pastime are fitted to the observed distributions of household size, workplace size, and household trips, respectively (Fig. 5a–c). In addition, it has been reported that the average number of daily contacts of an individual is 16.8 in a survey of 92 adults (Edmunds, 1997), or near the

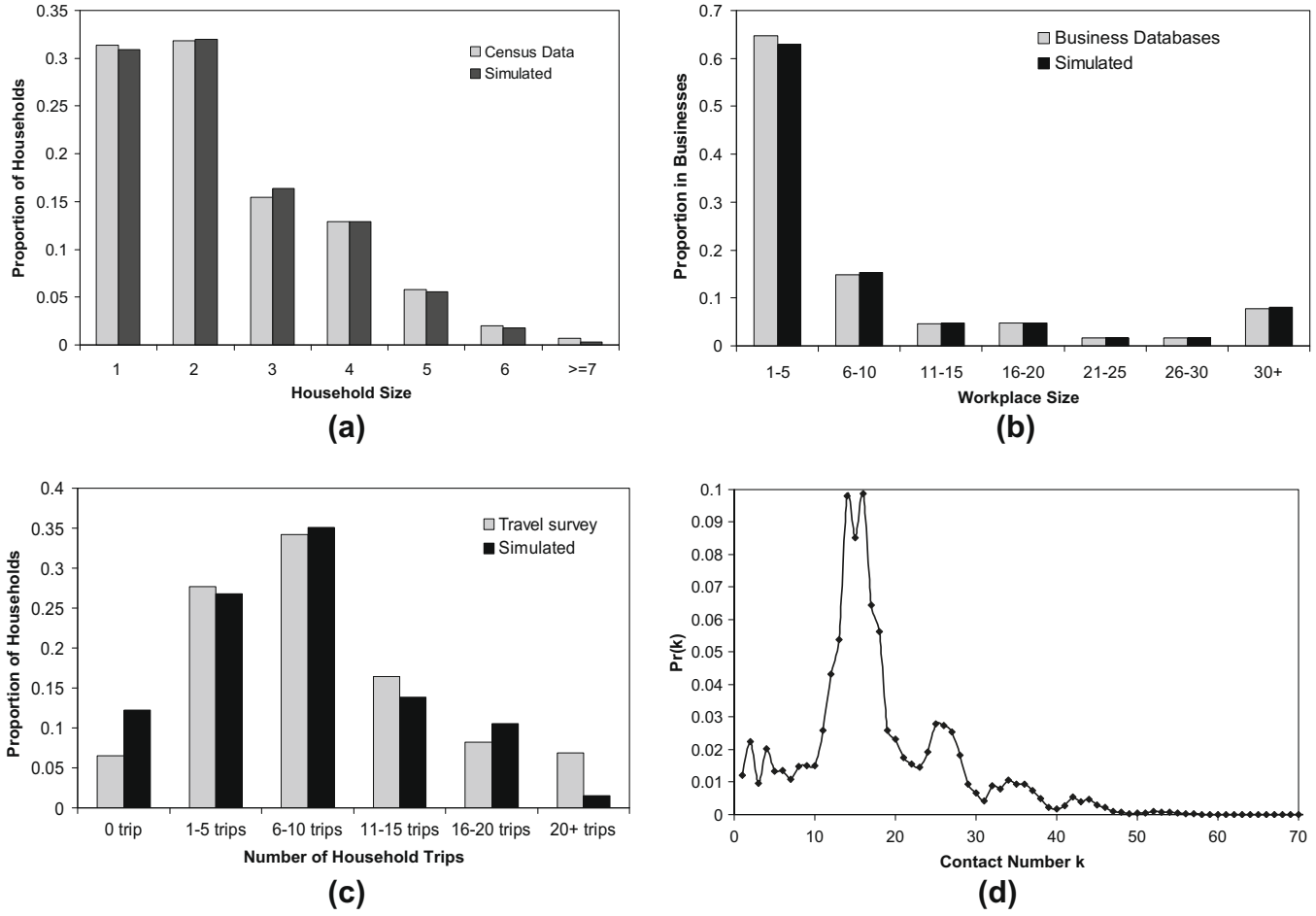

Fig. 5. The observed and fitted distribution of: (a) household size, (b) workplace size, and (c) household trips. (d) The probability distribution of daily contact numbers of all individuals. The average number of contacts of an individual is estimated to be 16.9.

midpoint of range 10–19 in surveys of Chinese society (Fu, 2005). Based on these two social studies, the maximum contacts of an individual at a service place is calibrated to two, and at this value, the simulated number of daily contacts of an individual is on average 16.9 (Fig. 5d).

To calibrate the age-specific infection rates I_{age}, three indices are estimated and compared to established literature, including a basic reproductive number (R_0), an overall attack rate, and proportions of infection by location. First, R_0 is the number of individuals in a susceptible population that are directly infected by the introduction of a single infectious individual (Diekmann, Heesterbeek, & Metz, 1990). Recent studies on observed data have reported that the R_0 of influenza ranges from 0.9 to 2.1 with a mean of 1.3 (Chowell, Miller, & Viboud, 2007; Ferguson et al., 2005; Mills, Robins, & Lipsitch, 2004). In this study, R_0 is estimated by tracing the number of infections directly caused by the infection sources. Second, the overall attack rate is the proportion of total population that is infected during an epidemic. The observed overall attack rate for influenza epidemics ranges from 10% to 20% of the population (CDC., 2008; Cox & Subbarao, 2000). Third, the proportion of infections at households (including homes and neighbor households), workplaces, and service places are estimated to be in the ranges of 47–51%, 37–42%, 11–12%, respectively (Longini & Halloran, 2005; Yang et al., 2008). To match the three indices to established literature (Table 3), the infection rates I_{age} for children, adults, and seniors are calibrated to 0.1, 0.08, and 0.09, respectively. In addition, the effectiveness of occasional contacts for infection $E_{ocassional\_contact}$ is calibrated to 0.2.

Table 3
The calibration of model outputs under four seeding scenarios to the literature.

	From literature	Random	CBD	Transition zone	Suburbs
R_0	1.3 (0.9–2.1)	1.38	1.39	1.30	1.52
Overall attack rate	10–20%	17.4%	16.4%	16.7%	17.7%
% of infection at households	47–51%	49.1%	49.3%	48.2%	49.1%
% of infection at workplaces	37–42%	39.1%	38.9%	39.1%	39.1%
% of infection at service places	11–12%	11.8%	11.8%	12.7%	11.8%

To validate the model, weekly reports of laboratory confirmed specimens in the 2004–2005 influenza season are collected from New York State Department of Health (NYSDOH, 2005). As shown in Fig. 6, the time course of the epidemic is well predicted by the model, although the magnitude of simulated cases is much larger than the laboratory data. The first possible reason is that a large number of infected individuals (more than 80%) may choose self-care and are reluctant to seek health care (McIsaac, Levine, & Goel, 1998; Stoller et al., 1993). These infected individuals cannot be identified and reported. Second, for those who seek health care, only a small portion of their specimens are submitted for laboratory testing. Therefore, the number of influenza cases is always highly under-reported, and a complete data is rather difficult to collect. The laboratory data, so far, may be the best available touchstone for model validation. In this sense, our model performs well

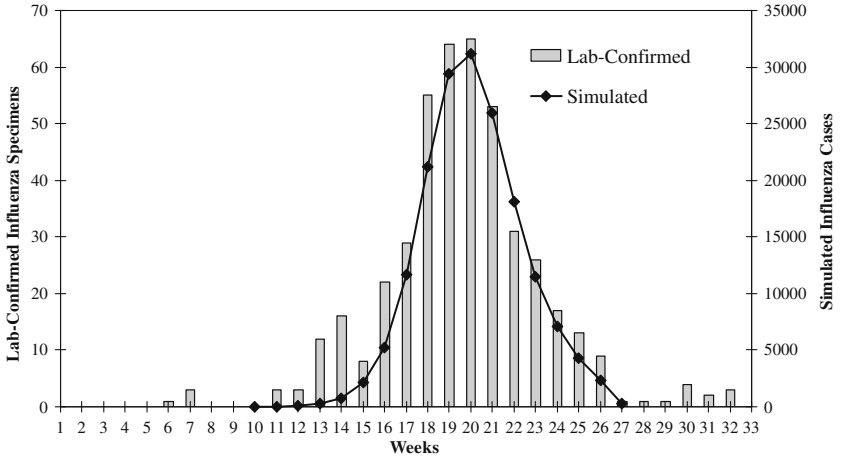

Fig. 6. The validation of simulation results by the weekly laboratory confirmed influenza specimens in Season 2004–2005. The time course of the epidemic well matches the observed records, although the absolute number of cases is much larger than the observed cases. This is reasonable because the influenza cases are always highly under-reported.

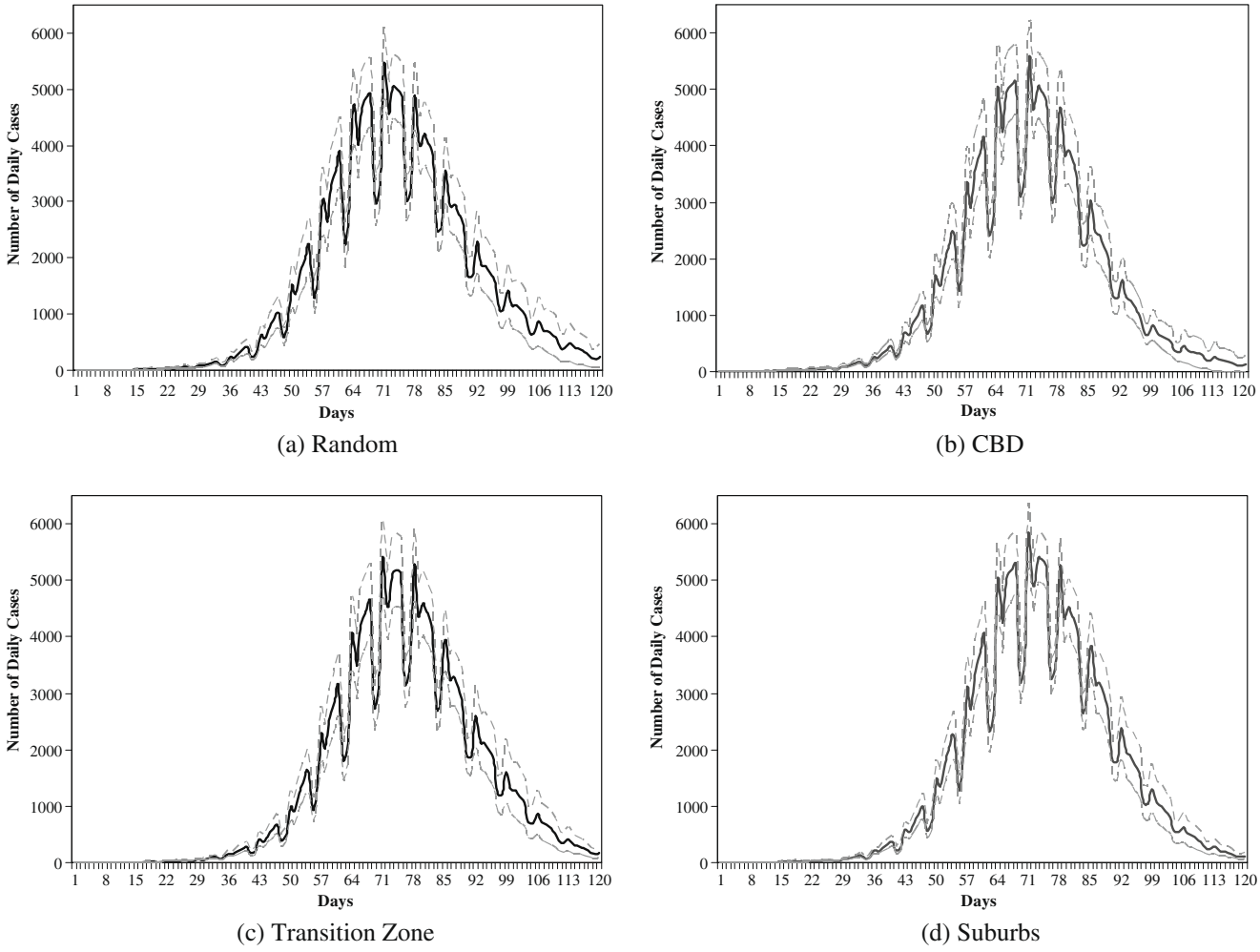

Fig. 7. The epidemic curves under the four seeding scenarios. The solid curves represent the average number of daily new cases (symptomatic individuals) by 50 simulations, while the dash curves represent the 95% confidence intervals.

in predicting the trend, and at least allows the estimate of a worse case result.

The calibration and validation indicate that the established model is a close representation of influenza transmission. Based on this model, the information about every infection event can be traced, such as who infects whom, and where and when the infection occurs. This information provides detailed clues for analyzing the spatial–temporal transmission of influenza.

4.2. Time sequence of influenza transmission

The epidemic curves in Fig. 7 indicate similar temporal dynamics of influenza transmission under the four seeding scenarios. No matter where the infection sources are initially distributed, the influenza epidemic develops similarly with respect to the peak time, peak number of new cases, and total number of cases. The epidemic curves start with a very slow increase as time proceeds to Day 40 with a cumulative number of influenza cases around 2800 (2.84‰ of the population). An abrupt rise begins approximately after Day 40, and subsequently the number of daily new cases peaks at around Day 70. The average peak number is 5450 new cases, about 5.54‰ of the population. After the peak, the number of daily new cases drops quickly until the end of the epidemic. It is worth mentioning that the number of daily new cases is cyclical over time, increasing during weekdays and decreasing during weekends. This results in a bumpy curve rather than a smooth one.

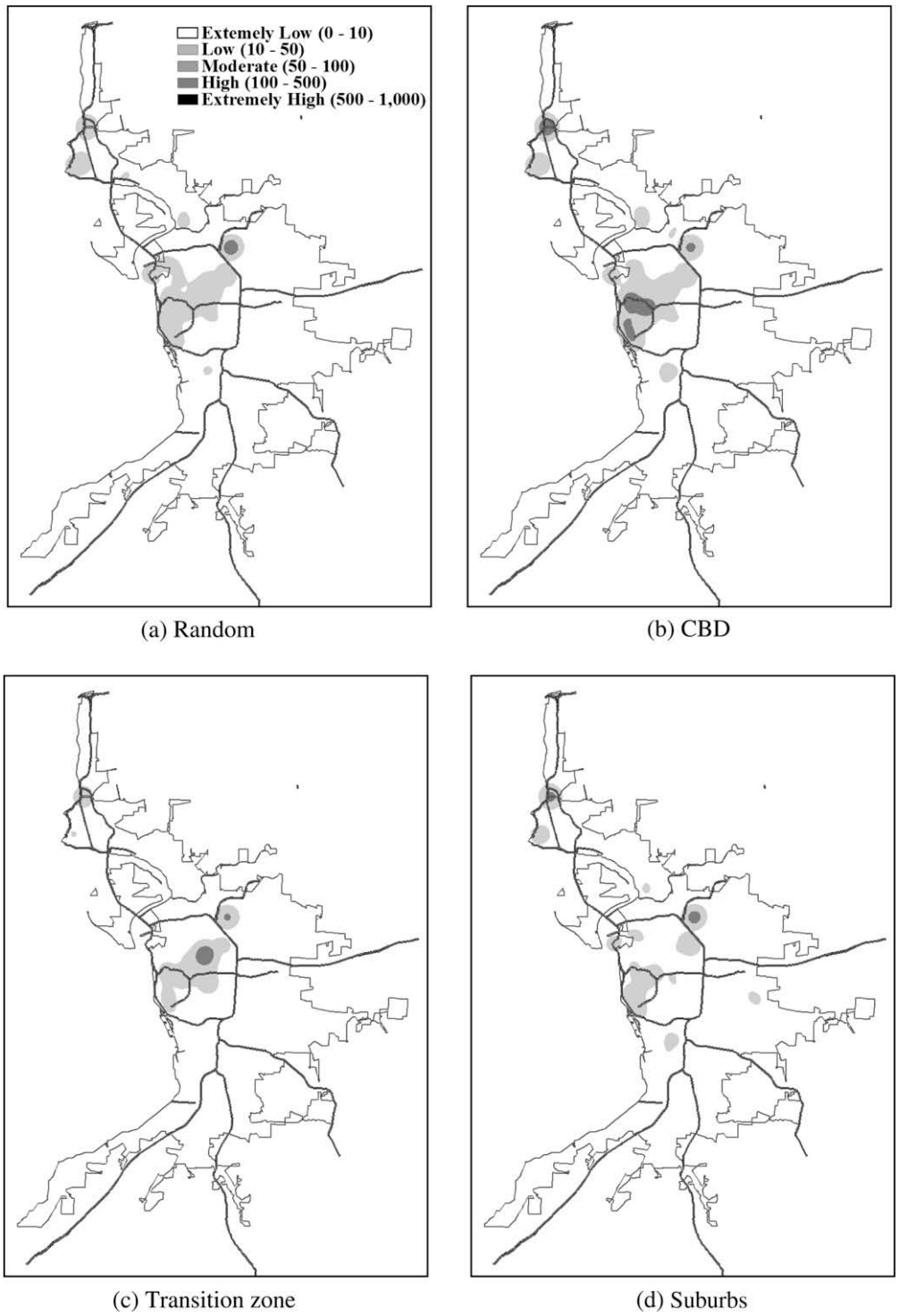

Fig. 8. (a)–(d) display the spatial spread of influenza during Days 1–40 under the random, CBD, transition zone, and suburbs seeding scenarios, respectively. The gray-scale color represents the infection intensity (number of new infections per sq km^2) at a cell location, with the highest in black and the lowest in white.

4.3. Spatial spread of influenza

The spatial spread of influenza is of interest. In Figs. 8 and 9, the infection intensity at each cell location is categorized into five levels: extremely low (0–10 infections/sq km^2), low (10–50), moderate (50–100), high (100–500), and extremely high (500–1000). For the first 40 days, the four seeding scenarios produce different spatial patterns of infection. As shown in Fig. 8, the infections tend to be limited to areas around the seeding locations, producing moderate infection intensity. In addition, there are a few low-intensity areas distant from the seeding locations, most likely to occur within the downtown Buffalo, the downtown Niagara Falls, the University of Buffalo, and the Niagara University. After Day 40, as the number of new infections increases exponentially, the spatial spread of influenza tends to be similar for all four seeding scenarios. For this reason, Fig. 9 only displays the spatial spread of influenza under the random seeding scenario, while the other three scenarios are reported in the supplementary document. Be-

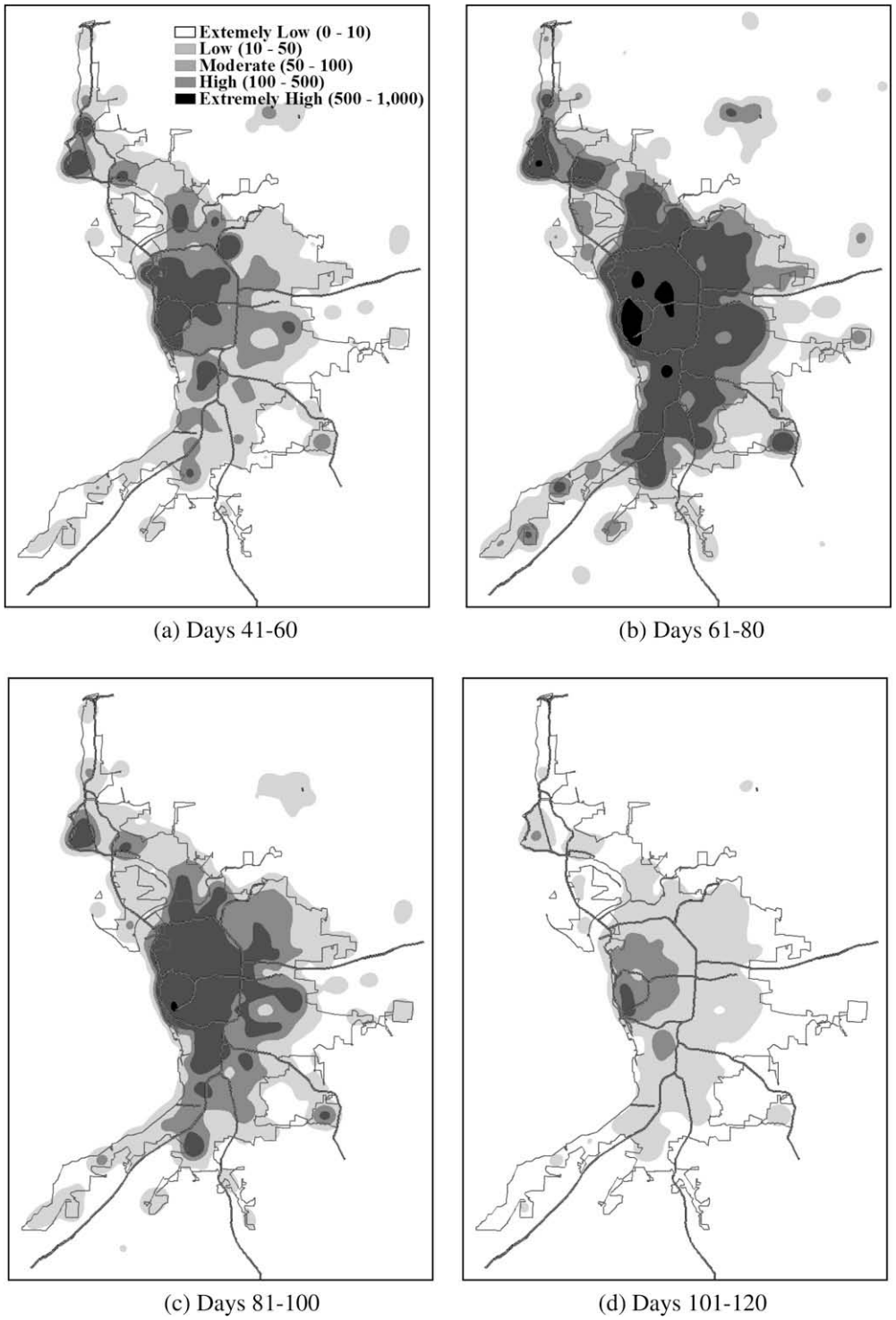

Fig. 9. (a)–(d) DISPLAY the spatial spread of influenza between Days 41–60, Days 61–80, Days 81–100, and Days 101–120, respectively. The gray-scale color represents the infection intensity at a cell location (number of new infections per sq km^2), with the highest in black and the lowest in white.

tween Days 41 and 60 (Fig. 9a), the infections span long distances and the epidemic rapidly transforms from being predominantly local to city-wide. High infection intensity begins to occur in the CBD and transition zone, while low infection intensity covers the entire suburbs.

From Days 61 to 80 (Fig. 9b), the entire study area is undergoing a fast and heterogeneous growth in infections. Five areas with extremely high-intensity values are identified, including the downtown Buffalo, the south campus of University of Buffalo, the town center of Kenmore, the industrial area in southern Buffalo, and the downtown Niagara Falls (ordered by the spatial extent from the largest to the smallest). The remaining areas, covering most parts of the transition zone and suburbs, are dominated by high infection intensity. From Days 81 to 100 (Fig. 9c), the spatial extent of high infection intensity gradually recedes to the transition zone, leaving the suburbs with moderate or low infection intensity. In the final 20 days (Days 101–120), only a small area in the CBD retains high-intensity infection (Fig. 9d). For the remaining areas, the intensity decreases rapidly from the transition zone to the suburbs.

5. Discussion

The epidemic curves in Fig. 7 imply that the first month of a flu season (before Day 40) would be crucial for influenza control and prevention. This is because the number of influenza cases increases slowly before Day 40, and the response time is relatively sufficient. The epidemic can potentially be avoided by applying voluntary control strategies, such as mass vaccination programs, and campaigns that promote preventive behaviors. If the early control cannot be achieved, the number of cases would increase dramatically. Under this circumstance, mandatory control strategies, such as case isolation, contact tracing, and household quarantine, should be implemented to mitigate the impacts of the epidemic. The weekly variation in the epidemic curves also suggests a possible control strategy that extends the weekend period by 1 or 2 days. Because most workplaces and schools are closed simultaneously during the weekends, fewer close contacts may occur than those in weekdays, resulting in fewer infections. The effectiveness of this weekend extension strategy is worthy of investigation.

The infection intensity maps (Figs. 8 and 9) indicate that the spatial spread of influenza can be described by five subsequent stages: local growth, expansion, fast city-wide growth, slow city-wide growth, and fade-out. The "growth", here, means the number of infections increases. As described in the Results section, the early influenza infections are focused around the infection sources (local growth). Next, the new infections rapidly spread over the entire study area (expansion), probably because of the frequent travel of individuals between the CBD, transition zone, and suburbs. Subsequently, most locations in the study area experience a rapid and heterogeneous growth in infections (fast city-wide growth). As time proceeds, the growth of infections remains widespread but starts to slow down (slow city-wide growth). Finally, the growth of infections at every location fades out, possibly due to the herd immunity provided by recovered individuals.

This five-stage spreading process implies the existence of high-risk times and places in the study area. High-risk times occur when the total number of infections rises significantly, or when the spatial extent of affected areas expands rapidly. Days 41–60 and Days 61–80 are two high-risk time periods corresponding to the stages of expansion and fast city-wide growth, respectively. On the other hand, high-risk places can be identified as areas with extremely high intensity of infection. The downtown areas of both cities are at high risk because they have the highest densities of residents and businesses. Similarly, the town center of Kenmore is also suggested to be a high-risk place because of its intensive land use for residences, commerce and industry. The university campuses are large groups of individuals with dense within-group contacts, and they thus are at high risk. Likewise, the industrial park in southern Buffalo is another high-risk place, because it is a cluster of large-scale chemical factories with a large number of workers. Once influenza is identified in the study area, these high-risk places should be monitored under close surveillance and be targeted by control efforts with priority.

In summary, the spatial–temporal transmission of influenza and the resulting health risks can be attributed to two major and one minor factor. One of the two major factors is the spatial heterogeneity in the city, in terms of the population distribution and land use patterns (households and businesses). This factor directly influences the spatial layout of disease transmission. Areas with dense population or intensive land use patterns always end up with a high intensity of infection, while sparsely populated areas have relatively low intensity. The other major factor is the travel of individuals in the city, which has a profound effect on the temporal sequence of transmission. Without frequent travel of individuals between the CBD, transition zone, and suburbs, the infection can only expand locally around the infection sources. The city-wide travel of individuals quickly transports influenza viruses to everywhere else, leading to the rapid expansion of affected areas.

The one minor factor is the initial distribution of the infection sources. Regardless of where the infection sources are seeded, both the spatial layout and the temporal sequence of influenza transmission are similar, except for the early stage. It is intuitive that the spatial layout of transmission is similar under different seeding scenarios, because it is primarily determined by the inherent population distribution and land use patterns. Surprisingly, the temporal sequence of transmission also remains similar, and is insensitive to where infection sources are seeded. A possible reason is that individuals commute frequently between the three zones of the city, and can easily reach everywhere in the study area. Once the infection sources infect a sufficient number of surrounding individuals, the influenza viruses can be transported to places of high risks, from where similar spatial–temporal patterns of infection start to occur. This finding implies that wherever the initial infections are found, the control plan does not need a major change, and the control efforts may be only applied at fixed times and places. Further investigations of this finding are warranted.

There are three limitations of this study due to the complex disease system in a city. First, the behaviors of susceptible individuals do not change during the epidemic. In reality, these individuals may be influenced by their contacts, and spontaneously take preventive behaviors to protect themselves. Second, the simulation of population involves the disaggregation of census data, and assumes independence between a few of demographic variables. This independence assumption helps reduce the modeling complexity, but may also introduce biases in simulation. Existing individual data, such as Public Use Microdata Sample (PUMS), could be used to improve the simulation. Finally, this study assumes that immunity is obtained through early vaccination before the epidemic or through infection during the epidemic. It is also possible that individuals can gain immunity from previous epidemics, and therefore the immunity rate may be under-estimated. Although compensation for these limitations may improve the results, it also greatly increases the complexity of the model. It has been argued that the goal of modeling is not to predict exactly what may happen during an epidemic, but rather to observe how the epidemic may proceed and encourage appropriate questions. In this sense, the model results provide valuable knowledge regarding city-wide influenza transmission.

6. Conclusions and implications

This study contributes to the knowledge regarding influenza transmission at the city-wide scale, a topic that is under-studied in the current literature. An individual-based spatially explicit model has been developed to simulate influenza transmission through an urban contact network. The simulation results indicate a complex pattern of influenza transmission in a five-stage process. The complexity is attributable to three factors: the spatial heterogeneity in the population, the frequent city-wide travel of individuals, and the distribution of infection sources. The first factor primarily contributes to the spatial layout of disease transmission, while the second has a profound effect on the temporal sequence of transmission. The third factor, the infection–source distribution, only affects spatial–temporal transmission at the early stage, but its effect is largely weakened later by the city-wide travel of individuals. Therefore, the high risks of infection occur not only at the same locations, but also at almost the same times, regardless of where the infection sources are introduced. A number of studies may have reported the spatial similarity in high-risk places, but the temporal similarity has not been revealed before this study.

These results suggest a feasibility of identifying high-risk areas in advance based on analysis of census and land use data. These high-risk places should be set up as control targets during an epidemic wherever the initial infections are found. In addition, the results also imply that the incorporation of city-wide individual travel data into health surveillance is critical for designing proper timelines for allocating control efforts. These suggestions are particularly significant under the current circumstances in which vaccines and manpower are insufficient to combat the new wave of H1N1 influenza.

Appendix A. Supplementary material

Supplementary data associated with this article can be found, in the online version, at doi:10.1016/j.compenvurbsys.2010.03.004.

References

Anderson, R. M., & May, R. M. (1992). *Infectious diseases of humans: Dynamics and control*. New York: Oxford University Press.

Bian, L. (2004). A conceptual framework for an individual-based spatially explicit epidemiological model. *Environment and Planning B, 31*(3), 381–395.

Bian, L., Whalen, T., Cohen, M., Huang, Y., Lee, G., Lim, E., et al. (2008). Explicit spatial-temporal simulation of a rare disease. In *Paper presented at the Proceedings of the 11th Joint Conference on Information Sciences*, Shenzhen, China, December 15–20.

Carley, K. M., Fridsma, D. B., Casman, E., Yahja, A., Altman, N., Chen, L. C., et al. (2006). BioWar: Scalable agent-based model of bioattacks. *IEEE Transactions on Systems, Man and Cybernetics, Part A, 36*(2), 252–265.

CDC. (2008). Key facts about seasonal influenza (Flu). <http://www.cdc.gov/flu/about/disease/index.htm> Retrieved January, 2009.

Chowell, G., Miller, M. A., & Viboud, C. (2007). Seasonal influenza in the United States, France, and Australia: Transmission and prospects for control. *Epidemiology and Infection, 136*(6), 852–864.

Coburn, B. J., Wagner, B. G., & Blower, S. (2009). Modeling influenza epidemics and pandemics: Insights into the future of swine flu (H1N1). *BMC Medicine, 7*(30), 1–8.

Cox, N. J., & Subbarao, K. (2000). Global epidemiology of influenza: Past and present. *Annual Reviews in Medicine, 51*(1), 407–421.

Diekmann, O., Heesterbeek, J. A. P., & Metz, J. A. J. (1990). On the definition and the computation of the basic reproduction ratio R_0 in models for infectious diseases in heterogeneous populations. *Journal of Mathematical Biology, 28*(4), 365–382.

Edmunds, W. J. (1997). Who mixes with whom? A method to determine the contact patterns of adults that may lead to the spread of airborne infections. *Proceedings of the Royal Society B: Biological Sciences, 264*(1384), 949–957.

Eubank, S. (2005). Network based models of infectious disease spread. *Japanese Journal of Infectious Diseases, 58*(6), 9–13.

Eubank, S., Guclu, H., Anil Kumar, V. S., Marathe, M. V., Srinivasan, A., Toroczkai, Z., et al. (2004). Modelling disease outbreaks in realistic urban social networks. *Nature, 429*(6988), 180–184.

Euler, G. L., Bridges, C. B., Brown, C. J., Lu, P. J., Singleton, J., Stokley, S., et al. (2005). Estimated influenza vaccination coverage among adults and children-United States, September 1, 2004–January 31, 2005. *Morbidity and Mortality Weekly Report, 54*(12), 304–307.

Ferguson, N. M., Cummings, D. A. T., Cauchemez, S., Fraser, C., Riley, S., Meeyai, A., et al. (2005). Strategies for containing an emerging influenza pandemic in Southeast Asia. *Nature, 437*(7056), 209–214.

Fu, Y. (2005). Measuring personal networks with daily contacts: A single-item survey question and the contact diary. *Social Networks, 27*(3), 169–186.

GBNRTC. (2002). *Greater Buffalo-Niagara Regional Transportation Council*: 2002 *Regional Transportation Survey Results Report*. Buffalo, NY.

Germann, T. C., Kadau, K., Longini, I. M., Jr., & Macken, C. A. (2006). Mitigation strategies for pandemic influenza in the United States. *Proceedings of the National Academy of Sciences, 103*(15), 5935–5940.

Gordis, L. (2000). *Epidemiology*. Philadelphia: WB Saunders.

Grenfell, B. T., Bjornstad, O. N., & Kappey, J. (2001). Travelling waves and spatial hierarchies in measles epidemics. *Nature, 414*(6865), 716–723.

Grimm, V., & Railsback, S. F. (2005). *Individual-based Modeling and Ecology*. Princeton: Princeton University Press.

Halloran, M. E., Ferguson, N. M., Eubank, S., Ira, M., Longini, J., Cummings, D. A. T., et al. (2008). Modeling targeted layered containment of an influenza pandemic in the United States. *Proceedings of the National Academy of Sciences, 105*(12), 4639–4644.

Heymann, D. L. (2004). *Control of Communicable Diseases Manual* (18th ed.). Washington, DC: American Public Health Association.

Huang, C. Y., Sun, C. T., Hsieh, J. L., & Lin, H. (2004). Simulating SARS: Small-world epidemiological modeling and public health policy assessments. *Journal of Artificial Societies and Social Simulation, 7*(4).

Judson, O. P. (1994). The rise of the individual-based model in ecology. *Trends in Ecology & Evolution, 9*(1), 9–14.

Keeling, M. J. (1999). The effects of local spatial structure on epidemiological invasions. *Proceedings of the Royal Society B: Biological Sciences, 266*(1421), 859–867.

Keeling, M. J., & Eames, K. T. D. (2005). Networks and epidemic models. *Journal of the Royal Society Interface, 2*(4), 295–307.

Keeling, M. J., Woolhouse, M. E. J., Shaw, D. J., Matthews, L., Chase-Topping, M., Haydon, D. T., et al. (2001). Dynamics of the 2001 UK foot and mouth epidemic: Stochastic dispersal in a heterogeneous landscape. *Science, 294*(5543), 813–817.

Knox, P. L., & Marston, S. A. (2004). *Places and regions in global context: Human geography*. New Jersey: Prentice Hall.

Koopman, J. S. (2002). Controlling smallpox. *Science, 298*(5597), 1342–1344.

Koopman, J. S., & Lynch, J. W. (1999). Individual causal models and population system models in epidemiology. *American Journal of Public Health, 89*(8), 1170–1174.

Lee, B., Bedford, V. L., Roberts, M. S., & Carley, K. M. (2008). Virtual epidemic in a virtual city: Simulating the spread of influenza in a United States metropolitan area. *Translational Research, 151*(6), 275–287.

Longini, I. M., & Halloran, M. E. (2005). Strategy for distribution of influenza vaccine to high-risk groups and children. *American Journal of Epidemiology, 161*(4), 303–306.

Longini, I. M., Nizam, A., Xu, S., Ungchusak, K., Hanshaoworakul, W., Cummings, D. A. T., et al. (2005). Containing pandemic influenza at the source. *Science, 309*(5737), 1083–1087.

McIsaac, W. J., Levine, N., & Goel, V. (1998). Visits by adults to family physicians for the common cold. *Journal of Family Practice, 47*(5), 366–369.

Meade, M. S., & Earickson, R. J. (2005). *Medical geography*. New York: The Guilford Press.

Metzger, K. B., Hajat, A., Crawford, M., & Mostashari, F. (2004). How many illnesses does one emergency department visit represent? Using a population-based telephone survey to estimate the syndromic multiplier. *Morbidity and Mortality Weekly Report, 53*, 106–111.

Mills, C. E., Robins, J. M., & Lipsitch, M. (2004). Transmissibility of 1918 pandemic influenza. *Nature, 432*(7019), 904–906.

Molinari, N. A. M., Ortega-Sanchez, I. R., Messonnier, M. L., Thompson, W. W., Wortley, P. M., Weintraub, E., et al. (2007). The annual impact of seasonal influenza in the US: Measuring disease burden and costs. *Vaccine, 25*(27), 5086–5096.

NYSDOH. (2005). 2004–2005 Influenza season statewide summary report. <http://www.health.state.ny.us/diseases/communicable/influenza/surveillance/> Retrieved 2009.

New York State GIS Clearinghouse. (2009). Parcel data by town, city, and village. <http://www.nysgis.state.ny.us/>.

ReferenceUSA, Inc. (2009). US business databases. <http://www.referenceusa.com/Static/Home#businessDatabases>.

Riley, S., & Ferguson, N. M. (2006). Smallpox transmission and control: Spatial dynamics in Great Britain. *Proceedings of the National Academy of Sciences, 103*(33), 12637.

Stoller, E. P., Forster, L. E., & Portugal, S. (1993). Self-care responses to symptoms by older people. A health diary study of illness behavior. *Medical Care, 31*(1), 24–42.

Thompson, W. W., Shay, D. K., Weintraub, E., Brammer, L., Bridges, C. B., Cox, N. J., et al. (2004). Influenza-associated hospitalizations in the United States. *The Journal of the American Medical Association, 292*(11), 1333–1340.

US Census. (2000). Census 2000 data releases. <http://www.census.gov/main/www/cen2000.html>.

Wasserman, S., & Faust, K. (1994). *Social network analysis: Methods and applications*. Cambridge: Cambridge University Press.

Webby, R. J., & Webster, R. G. (2003). Are we ready for pandemic influenza? *Science, 302*(5650), 1519–1522.

Yang, Y., & Atkinson, P. M. (2008). Individual space–time activity-based model: A model for the simulation of airborne infectious-disease transmission by activity-bundle simulation. *Environment and Planning B: Planning and Design, 35*(1), 80–99.

Yang, Y., Atkinson, P., & Ettema, D. (2008). Individual space–time activity-based modelling of infectious disease transmission within a city. *Journal of the Royal Society Interface, 5*(24), 759–772.